

# Nonlinear bandgap transmission by discrete rogue waves induced in a pendulum chain

A. B. Togueu Motcheyo<sup>1,2,\*</sup>, Masayuki Kimura<sup>3</sup>, Yusuke Doi<sup>4</sup>, Juan F. R. Archilla<sup>5</sup>

<sup>1</sup> Department of Mechanical Engineering, Higher Technical Teacher's Training College (ENSET) Ebolowa, University of Ebolowa, P.O. Box 886, Ebolowa-Cameroon

<sup>2</sup> Laboratory of Mechanics, Department of Physics, Faculty of Science, University of Yaounde I, P.O. Box 812, Yaounde, Cameroon

<sup>3</sup> Department of Electrical and Electronic Engineering, Faculty of Science and Engineering, Setsunan University, Japan

<sup>4</sup> Department of Mechanical Engineering, Graduate School of Engineering, Osaka University 2-1 Yamadaoka, Suita, Osaka 565-0871, Japan

<sup>5</sup> Group of Nonlinear Physics, Universidad de Sevilla, ETSI Informática, Avda Reina Mercedes s/n, 41012-Sevilla, Spain\*

We study numerically a discrete, nonlinear lattice, which is formed by a chain of pendula submitted to a harmonic-driving source with constant amplitude and parametrical excitation. A supratransmission phenomenon is obtained after the derivation of the homoclinic threshold for the case when the lattice is driven at one edge. The lattice traps gap solitons when the chain is subjected to a periodic horizontal displacement of the pivot. Discrete rogue waves are generated for the case when the pendulum is simultaneously driven and shaken. This work may pave the way for experimental generation of discrete rogue waves within simple devices.

Keywords: Discrete rogue wave, Nonlinear supratransmission, Nonlinear pendulum

## I. INTRODUCTION

Since the pioneering work by Geniet and Léon [1] on the nonlinear supratransmission phenomenon, the behavior of a plane wave within the forbidden band has fascinated a number of researchers. Nowadays, there is another important consequence of this phenomenon, which is the capacity to reveal the types of waves that can propagate in the dispersive nonlinear lattice with a periodically driven boundary edge. Breathers have been generated in mechanical systems [1–7], in the Fermi-Pasta-Ulam Tsingou (FPUT) model [8–10], in a discrete inductance-capacitance electrical line [11], in Josephson junctions [12], and in molecular dynamics models [13]. An envelope soliton has been created in optical waveguide arrays [14–16] and in electrical lattices [17, 18]. A train of dark solitons has been generated in a discrete Schrödinger lattice with cubic-quintic nonlinearity [19]. A travelling asymmetric bright soliton has been generated for the  $\alpha, \beta$ -FPUT [10]. Up to now, to the best of our knowledge, the transmission of gap solitons is done continuously in time due to the periodic excitation at the edge of the lattice. There exist waves that seem to appear out of nowhere and then vanish without a trace [20]. They are called rogue waves, a phenomenon that has been observed in water [21, 22], nonlinear optics [23], photonic lattices [24], metamaterials [25], and in beam-plasma interactions [26], to mention a few systems.

Generally, rogue waves occur within systems modeled by an analytical integrable equation. For the continuous integrable equations, we can name the Sine-Gordon

equation [27], the one-dimensional Nonlinear Schrödinger (NLS) equation [20, 21], the coupled NLS equation [28], the Coupled Higgs Equation [29], and the Sasa-Satsuma equation [30]. For the analytically integrable discrete equation, rogue waves have been found in the discrete Ablowitz-Ladik [31], the coupled Ablowitz-Ladik equations [32], and the Ablowitz-Musslimani equation [33]. For the non-analytical integrable discrete equation, rogue waves have been simulated numerically in the discrete NLS equations with cubic [34], and saturable [35] nonlinearities. We have recently pointed out the first idea for the creation of a rogue wave within a nonlinear band gap in the conference paper [36]. The purpose of this letter is to consider a way of creating discrete rogue waves using a relatively simple device.

The outline of the paper is the following: in Section II, we present the model under investigation. The homoclinic supratransmission threshold is derived for the discrete Sine-Gordon equation. In Section III, we numerically integrate the dimensionless equation governing the physical model. Firstly, the chain of discrete pendula is studied without the parametric excitation in order to validate the supratransmission threshold; secondly, the lattice is shaken without a driven edge and thirdly, the behavior of the lattice is observed with a shaken and a driven edge simultaneously. The spectral analysis for the latter system is also included. Section IV concludes the letter.

\* Corresponding author: alain.togueu@univ-yaounde1.cm;

Alternate electronic addresses:

abtogueu@yahoo.fr; alainbertrandtogueu@gmail.com

## II. MODEL AND SUPRATRANSMISSION THRESHOLD

### A. Model description

The model under consideration consists of a pendulum chain connected by torsional springs and subjected to a horizontal driving force with frequency  $\omega_d$  and amplitude  $A$ , as illustrated in Fig. 1 reproduced from Ref. [37]. Each rigid rod of length  $L$  supports the pendulum bob with mass  $M$  at its end. The experimental system for the pendulum chain shown in Fig. 1 had been proposed in Ref. [38]. The Lagrangian for a chain of pendula in absence of damping can be written as follows [37]:

$$\mathcal{L} = \sum_{n=1}^N \left\{ \frac{1}{2} I \dot{\theta}_n^2 + \frac{1}{2} \left( Ml + \frac{ml}{2} \right) g \cos(\theta_n) \right. \\ \left. + \frac{1}{2} \left( Ml + \frac{ml}{2} \right) \left[ 2A\omega_d \dot{\theta}_n \sin(\omega_d t_1) \cos(\theta_n) \right] \right. \\ \left. - \frac{1}{4} \beta \left[ (\theta_n - \theta_{n-1})^2 + (\theta_n - \theta_{n+1})^2 \right] \right\}, \quad (1)$$

with  $I = Ml^2 + \frac{1}{3}ml^2$ . The angle  $\theta_n$  measures the deviation from the vertical for the  $n$ th pendulum,  $\dot{\theta}_n$  is the corresponding angular speed,  $g$  denotes the acceleration due to gravity, and  $\beta$  is the linear coupling coefficient between pendula due to a torsion spring. The equation of motion for the  $n$ th pendulum, derived using the Euler-Lagrange's equation, is given by [38, 39]:

$$\ddot{\theta}_n - \frac{\beta}{I}(\theta_{n+1} + \theta_{n-1} - 2\theta_n) + \omega_0^2 \sin(\theta_n) + \\ f\omega_d^2 \cos(\omega_d t_1) \cos(\theta_n) = 0, \quad (2)$$

with  $\omega_0^2 = \frac{g}{I}(Ml + \frac{ml}{2})$ , and  $f = \frac{\omega_0^2 A}{g}$ , being the dimensionless forcing coefficient. Equation (2) can be further simplified by scaling the time using the transformation.  $t_1 = \frac{t}{\omega_0}$ . In this way, the dimensionless form of the equation of motion for the  $n$ th pendulum can be written as follows:

$$\ddot{\theta}_n - c(\theta_{n+1} + \theta_{n-1} - 2\theta_n) + \sin(\theta_n) + \\ f\omega_1^2 \cos(\omega_1 t) \cos(\theta_n) = 0, \quad (3)$$

where  $c = \frac{\beta}{I}$  is the dimensionless coupling parameter, and  $\omega_1 = \frac{\omega_d}{\omega_0}$  is the dimensionless frequency for the periodic horizontal displacement of the pivot. The linear dispersion relation for Eq. (3) is given by

$$\omega^2 = 1 + 2c(1 - \cos(k)), \quad (4)$$

from which the linear band  $1 \leq \omega \leq \sqrt{1 + 4c}$  is obtained.

### B. Supratransmission threshold

Here, we consider the model without the forcing coefficient, i.e.,  $f = 0$ , then Eq. (3) becomes the equation of

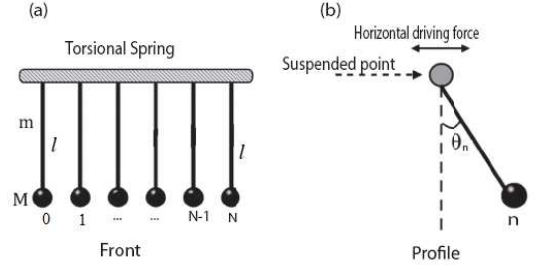


FIG. 1. Schematic representation of a pendulum chain connected by torsional springs subjected to a horizontal driving force. (a) front view; (b) profile view. Reproduced with permission from Ref. [37], copyright by APS 2014.

the Sine-Gordon pendulum. Expanding  $\sin(\theta_n)$  as a Taylor series up to the third order, the equations of motion become

$$\ddot{\theta}_n - c(\theta_{n+1} + \theta_{n-1} - 2\theta_n) + \theta_n - \frac{\theta_n^3}{6} = 0. \quad (5)$$

The time-periodic solution of the equation can be obtained by proposing a harmonic solution in the form  $\theta_n = x_n \cos(\omega t)$  (see Refs. [40–42]). The map corresponding to the stationary equation can be written as [40–48]

$$x_{n+1} = ax_n - bx_n^3 - y_n, \quad y_{n+1} = x_n. \quad (6)$$

with  $a = 2 + \frac{1}{c}(1 - \omega^2)$  and  $b = \frac{1}{8c}$ . This map possesses three fixed points:  $x_0 = 0$  and  $x_{\pm} = \pm\sqrt{8(1 - \omega^2)}$ . The latter two exist only for  $\omega < 1$ . This corresponds to the lower forbidden band and it in agreement with the band for which supratransmission phenomenon has been performed by Geniet and Léon [1]. Fixed points are depicted by a cross in Fig. 2. The stability of a fixed point is obtained by linearizing the map around the fixed point using the procedure described in Ref. [47]. A necessary condition for the existence of manifolds is that the fixed point must be a saddle point. A homoclinic orbit corresponds to an orbit that connects, both in forward and backward time, a saddle fixed point with itself [46]. Within the lower forbidden band ( $\omega < 1$ ) only the fixed point  $x_0 = 0$  is a saddle point. Figure 2 depicts the progression of the stable (blue line) and unstable (red line) manifolds emanating from the fixed point  $x_0 = 0$ . The corresponding main homoclinic connection can be clearly observed. The supratransmission threshold corresponds to the value of the turning point of the main homoclinic orbit [15]. Its value can be identified in this work by the dashed green line in Fig. 2.

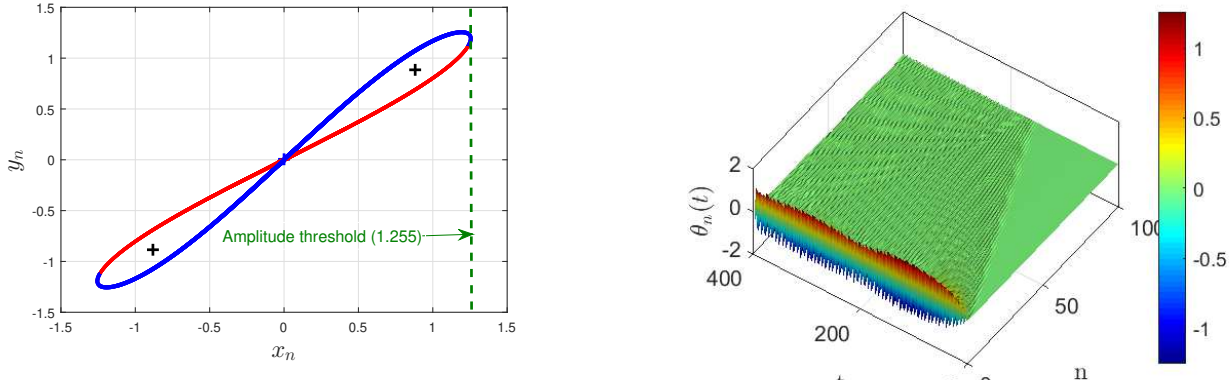


FIG. 2. Homoclinic orbit of the 2D map (6) for  $c = 1$ , and  $\omega = 0.95$ . The dashed green line corresponds to the supratransmission threshold:  $A_{thr} = 1.255$ .

### III. NUMERICAL EXPERIMENT

In this section, numerical studies are carried out on the discrete equation (3) with the ode45 solver of MatLab. This solver uses variable time step to keep the desired relative and absolute tolerance, which are set at  $10^{-10}$ . The left boundary of the lattice depends on whether or not the lattice is driven. The reflection at the right edge of the lattice will be avoided by choosing a large value of  $N$ , but only a few of them will be depicted after full integration of Eq. (3).

#### A. Driven Sine-Gordon pendulum

The unshaken lattice ( $f = 0$ ) will be considered here and the following harmonic boundary condition is imposed to the chain for the full integration of Eq. (3):

$$\theta_0(t) = A \cos(\omega t), \quad (7)$$

where  $A$  is the driving amplitude smoothly growing from the value 0 to  $A$  and  $\omega$  is the dimensionless frequency. Figure 3 depicts the behavior of the chain with driving amplitude  $A = 1.254$  (slightly below the threshold 1.255) and with the dimensionless frequency  $\omega = 0.95$  within the lower forbidden band, while Fig. 4 shows a train of gap solitons generated by driving the lattice with amplitude  $A = 1.256$  (slightly above the threshold 1.255) and the same frequency. The evanescent wave seen in Fig. 3 and the energy flow shown in Fig. 4 confirm the agreement of the homoclinic threshold shown in Fig 2 with the numerical simulation.

#### B. Horizontally shaken pendulum

The lattice is subjected to a periodic horizontal displacement of the pivot point with dimensionless fre-

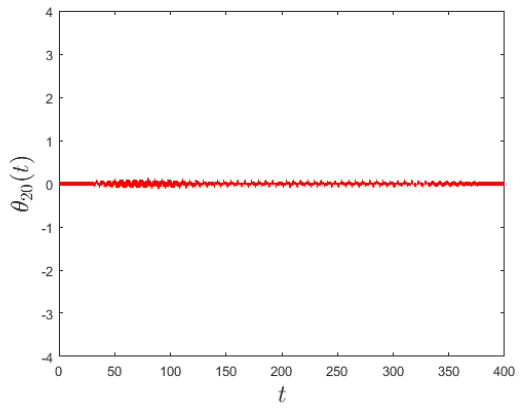


FIG. 3. Spatiotemporal evolution for the discrete equation (3) with boundary driving condition (7). The parameters are  $f = 0$ ,  $c = 1$ ,  $\omega = 0.95$ , and  $A = 1.254 < A_{thr}$

quency  $\omega_1$  and amplitude  $f$ . Figure 5 depicts the spatiotemporal evolution of the wave that results from the full integration of Eq. (3) with a shaking dimensionless frequency in the lower forbidden band ( $\omega_1 = 0.95$ ) and the other parameters given by:  $f = 0.2$  and  $c = 1$ . It is observed, similarly to Ref. [37], that the lattice traps the gap soliton and that, therefore, there is no transmission process. The same phenomenon is observed (not shown here) in the upper forbidden band. The trapping of the gap soliton here is done at different times, and the differences of localization in space are consequence to the staggeringly driving force obtained in Ref. [49]. Another form of localization can be obtained using random fluctuations [50]. By periodically driving the lattice, the gap transmission is observed while the soliton is trapped at a different time when the chain is subjected to a periodic horizontal shaking. Below, the behavior of the chain will be explored when it is subjected to being both simultaneously driven and shaken.

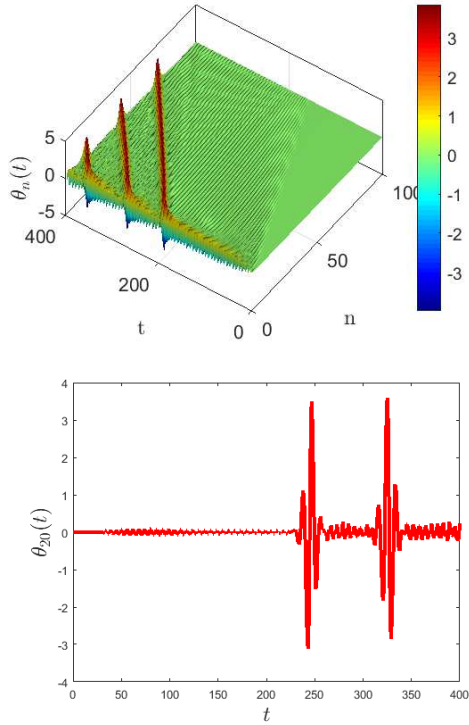


FIG. 4. Spatiotemporal evolution for the discrete equation (3) with boundary driving condition (7). The parameters are  $f = 0$ ,  $c = 1$ ,  $\omega = 0.95$ , and  $A = 1.256 > A_{thr}$ .

### C. Simultaneously driven and shaken model

Here we have two excitations: periodically driven edges and parametric excitation. The periodically driven edge frequency is taken in the lower forbidden band ( $\omega = 0.95$ ). The shaking frequency  $\omega_1$  will be taken firstly within the linear phonon band ( $1 \leq \omega \leq \sqrt{1+4c}$ ) and secondly in the lower forbidden band ( $\omega < 1$ ).

Figure 6 shows the spatiotemporal evolution of the chain with a driving frequency ( $\omega = 0.95$ ) within the lower forbidden band and driving amplitude ( $A = 1.22$ ) below the supratransmission threshold ( $A_{thr} = 1.255$ ). The shaking frequency ( $\omega_1 = 1.22$ ) is taken within the linear phonon band. The generation of a train of solitons is observed, although the driving amplitude is below the threshold. Therefore, the presence of the shaking reduces the supratransmission threshold. The same phenomenon is observed (not shown here) when the shaking frequency is taken in the upper forbidden band.

Let us now consider the case where the driving amplitude is  $A = 1.256 > A_{thr}$  and the frequency is  $\omega = 0.95$ . Without the shaking phenomenon ( $f = 0$ ), numerical integration of Eq. (3) with these parameters generates band-gap transmission as can be seen in Fig. 4. Figure 7 (a) shows that the presence of shaking with frequency  $\omega_1 = 0.8$ , within the lower forbidden band, destroys the supratransmission phenomenon. This is con-

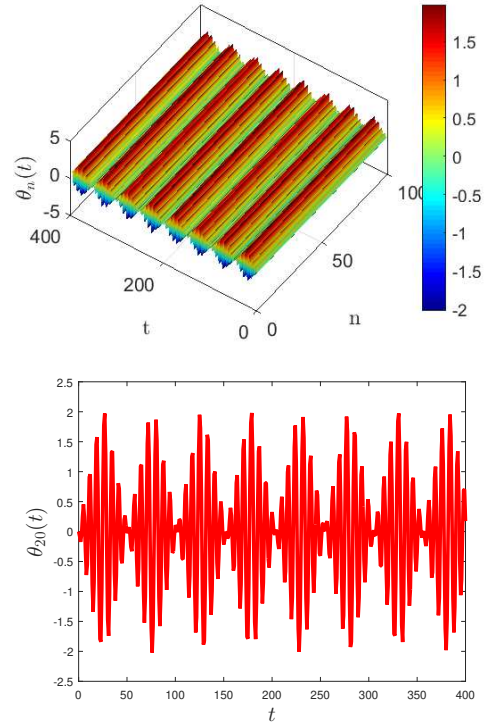


FIG. 5. Spatiotemporal evolution of the lattice submitted to periodic horizontal shaking:  $f = 0.2$ ;  $c = 1$ ;  $\omega_1 = 0.95$ .

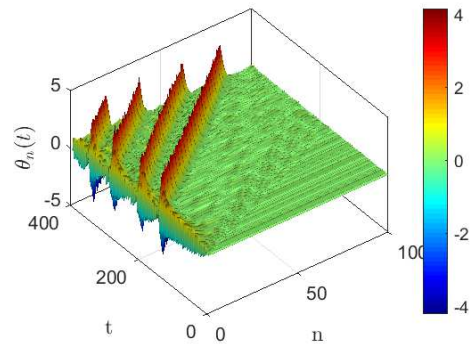


FIG. 6. Spatiotemporal evolution of the lattice with coupling constant  $c = 1$  submitted simultaneously to a periodically driven edge ( $\omega = 0.95$ ,  $A = 1.22 < A_{thr}$ ), and a periodic horizontal shaking with frequency  $\omega_1 = 1.22$  in the linear band. The forcing coefficient is  $f = 0.02$ .

trary to the case with the shaking frequency within the phonon band. When the forcing coefficient  $f$  increases to  $f = 0.08$ , the nonlinear bandgap transmission occurs as can be seen in Fig. 7 (b). The presence of the shaking phenomenon here increases the supratransmission threshold.

In Fig. 8, we depict a progression of the spatiotemporal evolution of the driven lattice in the presence of the

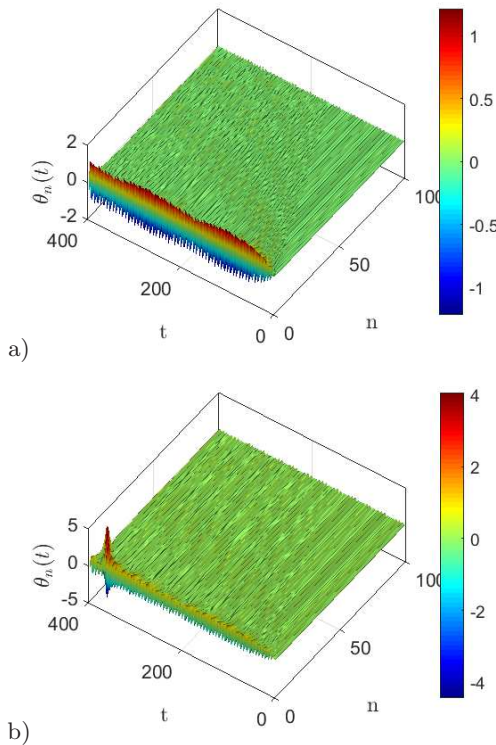


FIG. 7. Spatiotemporal evolution of the lattice with coupling constant  $c = 1$  submitted simultaneously to a periodically driven edge ( $\omega = 0.95$ ,  $A = 1.256 > A_{thr}$ ), and a periodic horizontal shaking frequency  $\omega_1 = 0.8$  in the lower forbidden band. Forcing coefficient: a)  $f = 0.02$ , b)  $f = 0.08$

#### D. Spectral analysis

We have performed the spectral analysis of rogue waves following Refs. [53]. In particular we present here the analysis of the case presented in Fig. 8 (d) for  $f = 0.03$ , where we can observe several rogue waves. As rogue waves are limited in time and space the precision of the two dimensional fast Fourier transform in space and time (XTFFT) is small as it depends on the time interval and sublattice size, which cannot be enlarged, but it provides valuable information nonetheless. For example, we concentrate in the rogue wave appearing in the first 30 particles for the time between 250 and 400, shown in Fig. 9 (a). The dispersion relation and the XTFFT are represented in Fig. 9 (b). The breather band can be seen slightly below the forcing frequency near  $k = 0$ . The corresponding breather line is also represented, its slope being the rogue wave velocity  $V_b \simeq 0.11$  which can also be obtained from the  $x(t)$  curve in Fig. 9 (a). The breather band value for  $k = 0$  provides the frequency in the moving frame  $\Omega_b \simeq 0.85$ . As this frequency is not zero, the rogue wave is breather-like and comparing  $\Omega_b$  with the velocity frequency  $\omega_V = 2\pi V_b$  (the frequency at which a rogue wave encounters different sites), we obtain that  $\Omega_b/\omega_V \simeq 5/4$ . This means that the rogue wave performs approximately 5 oscillations while moving 4 sites. As the

shaking phenomenon for different forcing coefficients  $f$ . The shaking frequency is equal to the driving frequency  $\omega$ . For small  $f$  ( $f = 0.02$ ), the band-gap transmission disappears, although the driving frequency is within the gap and the amplitude is above the supratransmission threshold, as can be seen in Fig. 8 (a). The disappearance of the supratransmission phenomenon means that the threshold increases in the presence of shaking with frequency within the lower forbidden band.

For  $f = 0.026$  (See Fig. 8 (b)), an unpredictable and unexpectedly localized wave appears and disappears without a trace. The phenomenon is similar to that obtained by Akhmediev et al. [20] in a continuous lattice. The discrete rogue wave is produced as a result of a simultaneously driven and shaken pendulum. For  $f = 0.027$  (Fig. 8 (c)), the number of unpredictable localized waves increases and the spatiotemporal dynamic of the lattice is similar to the second-order discrete rogue wave found analytically in Ref. [32]. For a slightly larger value of the forcing coefficient (see Fig. 8 (d)), several localized waves appear and the configuration is similar to that obtained in Ref. [51].

A discrete rogue wave is generated here with a plane wave as the initial condition. To the best of our knowledge, this is the first time that this phenomenon is observed.

central wave vector of the breather band is near  $k = 0$ , the different pendula have a small phase difference, meaning that the breather profile is bell shaped. Therefore, it is also confirmed that in this system rogue waves are below the phonon band. Similar analysis can be performed for other rogue waves with qualitatively similar results.

#### IV. CONCLUSION

In this work, we have studied the spatiotemporal behavior of the discrete pendulum chain, firstly excited by a harmonic wave, then by a parametric excitation, and finally by simultaneous driving and shaking excitations. The one-edge-driven lattice produces the well-known supratransmission phenomenon in agreement with the homoclinic threshold. Localization in space of the wave is obtained after shaking the lattice. The threshold of the supratransmission is reduced when the lattice is simultaneously driven with a frequency within the forbidden band and shaken with a frequency within the phonon band. The threshold value increases when it is shaken with a frequency in the lower forbidden band. Discrete rogue waves are obtained after simultaneously driving and shaking the lattice with the same frequency. The experimental device for the shaken pendulum has been realized in order to derive discrete breathers at Dickin-

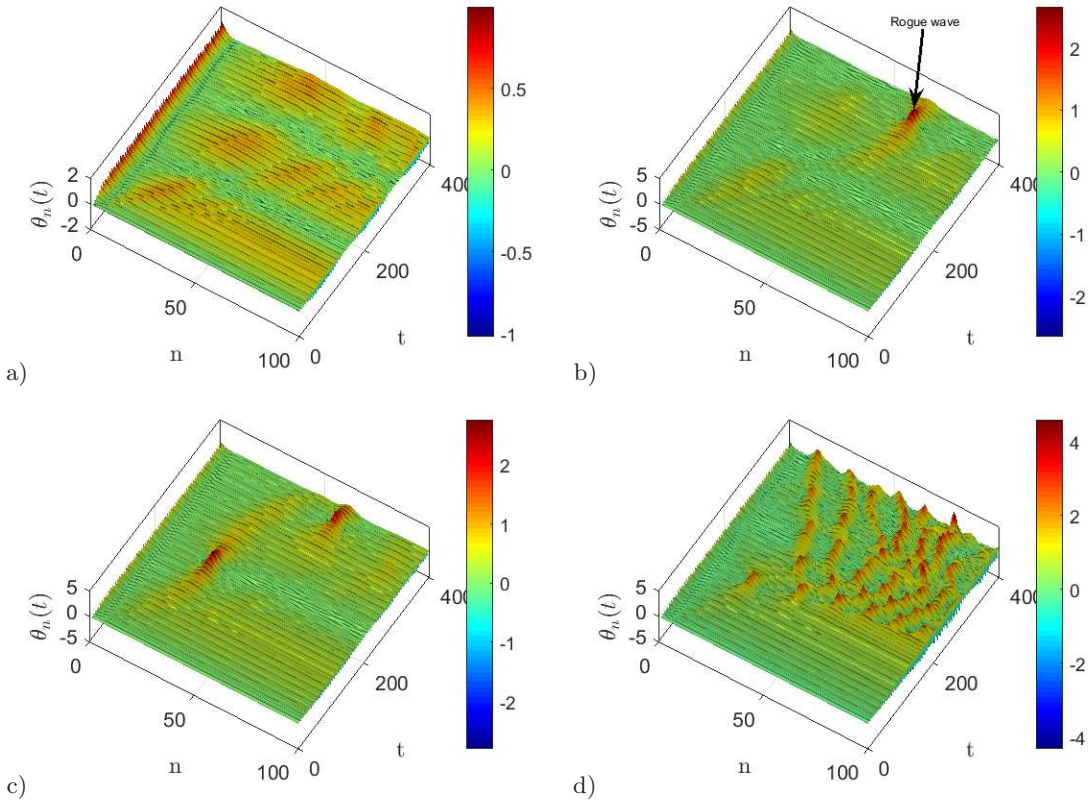


FIG. 8. Spatiotemporal evolution of the lattice with coupling constant  $c = 1$  submitted simultaneously to a periodically driven edge ( $\omega = 0.95$ ,  $A = 1.256$ ) and a periodic horizontal shaking ( $\omega_1 = \omega = 0.95$ ) with the forcing coefficient  $f$  increasing from left to right and from top to bottom: a)  $f = 0.02$ , b)  $f = 0.026$ , c)  $f = 0.027$ , d)  $f = 0.03$ .

son College [52]. We hope that the result presented in this letter will allow the modification of the experimental setup in order to obtain discrete rogue waves.

## ACKNOWLEDGMENTS

Alain Bertrand Togueu Motcheyo wishes to express its deepest gratitude to Prof. Masayuki Kimura and to all the organizers of the "International Symposium on Nonlinear Theory and Its Applications" (NOLTA 2022), December 12-15, 2022, for the opportunity they provided to

him for presenting a part of this work. JFRA acknowledges the Universities of Osaka and Latvia for hospitality.

## FUNDING

MK acknowledges support from grants JSPS Kakenhi (C) No. 21K03935. YD acknowledges the support from grant JSPS Kakenhi (C) No. 19K03654. JFRA thanks projects MICINN PID2019-109175GB-C22 and PID2022-138321NB-C22, and several travel grants from the VII PPITUS-2023 of the University of Sevilla.

---

[1] F. Geniet and J. Leon, Energy transmission in the forbidden band gap of a nonlinear chain, *Phys. Rev. Lett.* **89**, (2002) 134102.

[2] J. E. Macías-Díaz and A. Puri, On the propagation of binary signals in damped mechanical systems of oscillators, *Physica D* **228**, 112 (2007).

[3] J. E. Macías-Díaz, Numerical study of the transmission of energy in discrete arrays of sine-Gordon equations in two space dimensions, *Phys. Rev. E* **77**, (2008) 016602.

[4] J. E. Macías-Díaz, Numerical study of the process of nonlinear supratransmission in Riesz space-fractional sine-Gordon equations, *Commun. Nonlinear Sci.* **46**, (2017) 372 (2008) 5004.

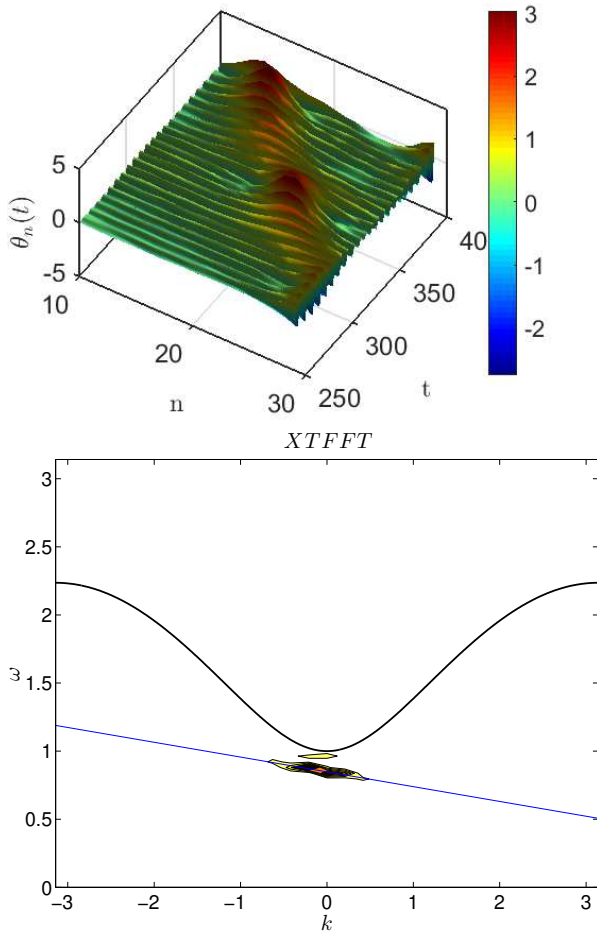


FIG. 9. **(Top)** Detail of the rogue wave observed in Fig. 8 (d). **(Bottom)** Frequency-momentum plot obtained using the two dimensional fast Fourier transform in space and time (XTFFT) for the first 30 sites and for a time between 250 and 400. The dispersion relation is shown for reference. The narrow band with constant slope corresponds to a breather with velocity  $V_b = \frac{\partial\omega}{\partial k}$ . The driving and shaking frequency appears as a faint short horizontal line just below the phonon band. See text and Refs. [53].

D. De Santis, C. Guarcello, B. Spagnolo, A. Carollo, D. Valenti, Supratransmission-induced traveling breathers in long Josephson junctions, *Commun. Nonlinear Sci.* **115**, (2022) 106736.

[5] Y. Watanabe, T. Nishida, Y. Doi, N. Sugimoto, Experimental demonstration of excitation and propagation of intrinsic localized modes in a mass-spring chain, *Phys. Lett. A* **382** (2018) 1957.

[6] J.E. Macías-Díaz and A.B. Togueu Motcheyo, Energy transmission in nonlinear chains of harmonic oscillators with long-range interactions, *Results in Physics* **18**, (2020) 103210.

[7] T. Bountis, K. Kaloudis, J. Shena, C. Skokos and C. Spitas, Energy transport in one-dimensional oscillator arrays with hysteretic damping, *Eur. Phys. J. Spec. Top.* **231**,

225 (2022);  
 Y. Wang, X. Zhang, S. Zhu Highly intensive and controllable supratransmission in a Kresling-origami metastructure, *Extreme Mech. Lett.* **59**, (2023), 101964;  
 Q. Zhang, H. Fang, and J. Xu, Programmable stopbands and supratransmission effects in a stacked Miura-Origami metastructure, *Phys. Rev. E* **101**, (2020) 042206;  
 M. J. Frazier, D. M. Kochmann, Band gap transmission in periodic bistable mechanical systems, *J. Sound. Vib.* **388**, (2017) 315;  
 A. Bader and O. V. Gendelman, Supratransmission in a vibro-impact chain, *J. Sound. Vib.* **547** (2023) 117493.

[8] R. Khomeriki, S. Lepri and S. Ruffo, Nonlinear supratransmission and bistability in the Fermi-Pasta-Ulam model, *Phys. Rev. E* **70**, (2004) 066626;  
 T. Dauxois, R. Khomeriki, S. Ruffo, Modulational instability in isolated and driven Fermi-Pasta-Ulam lattices, *Eur. Phys. J. Special Topics* **147**, (2007) 3;  
 J. E. Macías-Díaz, A. Bountis, Supratransmission in  $\beta$ -Fermi-Pasta-Ulam chains with different ranges of interactions, *CommunC Nonlinear Sci.* **63**, 307 (2018);  
 A. B. Togueu Motcheyo and J. E. Macías-Díaz, Energy transmission in the forbidden band-gap of a nonlinear chain with global interactions, *J. Phys. A: Math. Theor.* **53**, (2020) 505701;  
 S. D. Liazhkov, Energy supply into a semi-infinite  $\beta$ -Fermi-Pasta-Ulam-Tsingou chain by periodic force loading, *arXiv preprint arXiv:2212.09441* (2022).

[9] R. Alima, S. Morfu, P. Marquié, B. Bodo and B. Essimbi, Influence of a nonlinear coupling on the supratransmission effect in modified sine-gordon and klein-gordon lattices, *Chaos Sol. Fract.* **100**, (2017) 91.

[10] E. Nkendji Kenkeu, A. B. Togueu Motcheyo, Thomas Kanaa and C. Tchawoua, Wave propagation with longitudinal dust grain oscillations in dusty plasma crystals, *Phys. Plasmas* **29**, (2022) 043702

[11] K. Tse Ve Koon, J. Leon, P. Marquié, P. Tchofo-Dinda, Cutoff solitons and bistability of the discrete inductance-capacitance electrical line: Theory and experiments, *Phys. Rev. E* **75**, (2007) 066604;  
 K. Tse Ve Koon, P. Marquié, P. Tchofo Dinda, Experimental observation of the generation of cutoff solitons in a discrete LC nonlinear electrical line, *Phys. Rev. E* **90**, (2014) 052901;  
 S.B. Yamgoué, S. Morfu, P. Marquié, Noise effects on gap wave propagation in a nonlinear discrete LC transmission line. *Phys Rev E* **75**, (2007) 036211;  
 F. T. Ndjomatchoua, C. Tchawoua; F. M. M. Kakmeni, B. P. Le Ru, H. E. Z. Tonnang, Waves transmission and amplification in an electrical model of microtubules, *Chaos* **26**, (2016) 053111.

[12] D. De Santis, C. Guarcello, B. Spagnolo, A. Carollo, D. Valenti, Generation of travelling sine-Gordon breathers in noisy long Josephson junctions, *Chaos Sol. Fract.* **158**, (2022) 112039; J. E. Macías-Díaz, Persistence of nonlinear hysteresis in fractional models of Josephson transmission lines Author links open overlay panel, *CommunC Nonlinear Sci.* **53**, (2017) 31

[13] P.V. Zakharov, The effect of nonlinear supratransmission in discrete structures: a review, *Computer Research and modeling* **15**, no. 3 (2023) P. e599-e617;  
 P. V. Zakharov, E. A. Korznikova, A. A. Izosimov and A. S. Kochkin, The Influence of Crystal Anisotropy on the Characteristics of Solitary Waves in the Nonlinear

Supratransmission Effect: Molecular Dynamic Modeling, Computation **11**(10), (2023) 193.

[14] R. Khomeriki, Nonlinear band gap transmission in optical waveguide arrays, Phys. Rev. Lett. **92**, (2004) 063905.

[15] A. B. Togueu Motcheyo, J. D. Tchinang Tchameu, M. Siewe Siewe, C. Tchawoua, Homoclinic nonlinear band gap transmission threshold in discrete optical waveguide arrays, CommunC Nonlinear Sci. **50**, (2017) 29; A. B. Togueu Motcheyo, J. E. Macías-Díaz, Nonlinear bandgap transmission with zero frequency in a cross-stitch lattice, Chaos Sol. Fract. **170**, (2023) 113349.

[16] H. Susanto, Boundary driven waveguide arrays: supratransmission and saddle-node bifurcation, SIAM Journal on Applied Mathematics **69**, (2008) 111; H. Susanto, N. Karjanto, Calculated threshold of supratransmission phenomena in waveguide arrays with saturable nonlinearity, J. Nonlinear Opt. Phys. Mater **17**, (2008) 159.

[17] A. B. Togueu Motcheyo, C. Tchawoua, M. Siewe Siewe and J. D. Tchinang Tchameu, Supratransmission phenomenon in a discrete electrical lattice with nonlinear dispersion, Commun. Nonlinear Sci. **18**, (2013) 946.

[18] A. B. Togueu Motcheyo, C. Tchawoua, and J. D. Tchinang Tchameu, Supratransmission induced by waves collisions in a discrete electrical lattice, Phys. Rev. E **88**, (2013) 040901.

[19] A. B. Togueu Motcheyo, M. Kimura, Y. Doi and C. Tchawoua, Supratransmission in discrete one-dimensional lattices with the cubic-quintic nonlinearity, Nonlinear Dyn **95**, (2019) 2461.

[20] N. Akhmediev, A. Ankiewicz, M. Taki, Waves that appear from nowhere and disappear without a trace, Phys. Lett. A **373** (2009) 675  
N. Akhmediev, J.M. Soto-Crespo, A. Ankiewicz, Extreme waves that appear from nowhere: On the nature of rogue waves, Phys. Lett. A **373** (2009) 2137

[21] A. Chabchoub, N. P. Hoffmann, and N. Akhmediev, Rogue Wave Observation in a Water Wave Tank, Phys. Rev. Lett. **106**, (2011) 204502.

[22] A. Chabchoub, N. Hoffmann, M. Onorato, and N. Akhmediev, Super Rogue Waves: Observation of a Higher-Order Breather in Water Waves, Phys. Rev. X **2**, (2012) 011015;  
T. A. A. Adcock and P. H. Taylor, The physics of anomalous ('rogue') ocean waves, Rep. Prog. Phys. **77** (2014) 105901.

[23] M. Tlidi and M. Taki, Rogue waves in nonlinear optics, Advances in Optics and Photonics, **14** No. 1 (2022) 87 <https://doi.org/10.1364/AOP.438025>  
D. R. Solli, C. Ropers, P. Koonath, B. Jalali, Optical rogue waves, Nature **450**, (2007) 1054  
G. R. Kol, S. Takougang Kingni, P. Woafo, Rogue waves in Lugiato-Lefever equation with variable coefficients, Cent. Eur. J. Phys. **12**(11) (2014) 767  
D. D. Estelle Temgoua, M. B. Tchoula Tchokonte, and T. C. Kofane, Combined effects of nonparaxiality, optical activity, and walk-off on rogue wave propagation in optical fibers filled with chiral materials, Phys. Rev. E **97**, (2018) 042205  
A. Coillet, J. Dudley, G. Genty, L. Larger, and Yanne K. Chembo, Optical rogue waves in whispering-gallery-mode resonators, Phys. Rev. A **89**, (2014) 013835  
W.-P. Zhong, M. Beli, B. A. Malomed, T. Huang, Breather management in the derivative nonlinear Schrödinger equation with variable coefficients, Annals of Physics **355**, (2015) 313

[24] C. G. L. Tiofack, S. Coulibaly, M. Taki, S. De Bievre and G. Dujardin, Comb generation using multiple compression points of Peregrine rogue waves in periodically modulated nonlinear Schrödinger equations, Phys. Rev. A **92**, (2015) 043837

[25] J. Cuevas-Maraver, B. A. Malomed, P.G. Kevrekidis, D.J. Frantzeskakis, Stabilization of the Peregrine soliton and Kuznetsov-Ma breathers by means of nonlinearity and dispersion management, Phys. Lett. A **382** (2018) 968  
K. Sakkaravarthi, R. Babu Mareeswaran and T. Kanna, Engineering optical rogue waves and breathers in a coupled nonlinear Schrödinger system with four-wave mixing effect, Phys. Scr. **95** (2020) 095202

[26] C. B. Tabi, H. Tagwo, and T. C. Kofane, Modulational instability in nonlinear saturable media with competing nonlocal nonlinearity, Phys. Rev. E **106**, (2022) 054201  
C. D. Pelwan, A. Quandt, and R. Warmbier, Onset times of long-lived rogue waves in an optical waveguide array, J. Opt. Soc. Am. A **37**, (2020) Issue 11, pp. C67-C72  
C. Han-Peng, B. Tian, J. Chai, Z. Du, Composite rogue waves and modulation instability for the three-coupled Hirota system in an optical fiber, Opt. Eng. **56**(10), (2017) 106114

[27] D. Rivas, A. Szameit, R. A. Vicencio, Rogue waves in disordered 1D photonic lattices, Scientific Reports **10**, (2020) 13064  
B. G. Onana Essama, J. Atangana, F. Biya Motto, B. Mokhtari, N. C. Eddeqaqi, and T. C. Kofane, Rogue wave train generation in a metamaterial induced by cubic-quintic nonlinearities and second-order dispersion, Phys. Rev. E **90**, (2014) 032911  
S. A. T. Fonkoua, F. B. Pelap, G. R. Deffo and A. Fomethé, Rogue wave signals in a coupled anharmonic network: effects of the transverse direction, Eur. Phys. J. Plus **136**, (2021) 416

[28] G. P. Veldes, J. Borhanian, M. McKerr, V. Saxena, D. J. Frantzeskakis and I. Kourakis, Electromagnetic rogue waves in beam-plasma interactions, J. Opt. **15** (2013) 064003.

[29] C. Hou, L. Bu, F. Baronio, D. Mihalache, S. Chen, Sine-Gordon breathers and formation of extreme waves in self-induced transparency media, Rom. Rep. Phys **72**.1, (2020) 405

[30] F. Baronio, A. Degasperis, M. Conforti, and S. Wabnitz, Solutions of the Vector Nonlinear Schrödinger Equations: Evidence for Deterministic Rogue Waves, Phys. Rev. Lett. **109**, (2012) 044102  
R. Babu Mareeswaran, E. G. Charalampidis, T. Kanna, P. G. Kevrekidis, and D. J. Frantzeskakis, Vector rogue waves and dark-bright boomeronic solitons in autonomous and nonautonomous settings, Phys. Rev. E **90**, (2014) 042912

[31] G. Mu and Z. Qin, Rogue Waves for the Coupled Schrödinger-Boussinesq Equation and the Coupled Higgs Equation, J Phys Soc Jpn. **81** (2012) 084001  
N. Akhmediev, J.M. Soto-Crespo, N. Devine, N.P. Hoffmann, Rogue wave spectra of the Sasa-Satsuma equation, Physica D **294**, (2015) 37  
A. Ankiewicz, N. Akhmediev and J. M. Soto-Crespo, Discrete rogue waves of the Ablowitz-Ladik and Hirota equations, Phys. Rev. E **82**, (2010) 026602

Y. Ohta and J. Yang, General rogue waves in the focusing and defocusing Ablowitz–Ladik equations, *J. Phys. A: Math. Theor.* **47**, (2014) 255201

W. Xiao-Yong, Controllable Discrete Rogue Wave Solutions of the Ablowitz–Ladik Equation in Optics, *Commun. Theor. Phys.* **66** (2016) 29

[32] W. Xiao-Yong Wen, Z. Yan, and B. A. Malomed, Higher-order vector discrete rogue-wave states in the coupled Ablowitz–Ladik equations: Exact solutions and stability, *Chaos* **26**, (2016) 123110

[33] F. Yu, Dynamics of nonautonomous discrete rogue wave solutions for an Ablowitz–Musslimani equation with -symmetric potential, *Chaos* **27**, (2017) 023108

M. Li, S. Juan-Juan, T. Xu, Generation mechanism of rogue waves for the discrete nonlinear Schrödinger equation, *Appl. Math. Lett.* (2018), <https://doi.org/10.1016/j.aml.2018.03.018>

[34] S. Efe, C. Yuce, Discrete rogue waves in an array of waveguides, *Phys. Lett. A* **379** (2015) 1251

[35] J. D. Tchinang Tchameu, A. B. Togueu Motcheyo, C. Tchawoua, Biological multi-rogue waves in discrete nonlinear Schrödinger equation with saturable nonlinearities, *Phys. Lett. A* **380**, (2016) 3057;

M. Gupta, S. Malhotra, R. Gupta, Comparative Study of Rogue Wave Solutions for Autonomous and Non-autonomous Saturable Discrete Nonlinear Schrödinger Equation, *Int. J. Theor. Phys.* **62**, 105 (2023).

[36] A. B. Togueu Motcheyo, M. Kimura, Y. Doi, J. F. R. Archilla, Supratransmission-Induced Discrete Rogue Wave in Nonlinear Chain, *IEICE Proceedings Series* **71**, (2022) C5L-B-03 DOI:10.34385/proc.71.C5L-B-03

[37] Y. Xu, T. J. Alexander, H. Sidhu, and P. G. Kevrekidis, Instability dynamics and breather formation in a horizontally shaken pendulum chain, *Phys. Rev. E* **90** (2014) 042921.

[38] R. Basu Thakur, L. Q. English and A. J. Sievers, Driven intrinsic localized modes in a coupled pendulum array, *J. Phys. D: Appl. Phys.* **41** (2008) 015503.

[39] J. Cuevas, L. Q. English, P. G. Kevrekidis, and M. Anderson, Discrete breathers in a forced-damped array of coupled pendula: modeling, computation, and experiment, *Phys. Rev. Lett.* **102** (2009) 224101

[40] A. Kamdoum Kuitche, A.B. Togueu Motcheyo, Thomas Kanaa, C. Tchawoua, Supratransmission in transversely connected nonlinear pendulum pairs, *Chaos Sol. Fract.* **160** (2022) 112196.

[41] P. Panagopoulos, T. Bountis and C. Skokos, Existence and Stability of Localized Oscillations in 1-Dimensional Lattices With Soft-Spring and Hard-Spring Potentials, *J. Vib. Acoust.* **126**(4), (2004) 520.

[42] F. Romeo and G. Rega, Periodic and localized solutions in chains of oscillators with softening or hardening cubic nonlinearity, *Meccanica* **50**, (2015) 721.

[43] T. Bountis, H. W. Capel, M. Kollmann, J.C. Ross, J. M. Bergamin, J. P. Van der Weele, Multibreathers and homoclinic orbits in 1-dimensional nonlinear lattices, *Phys. Lett. A* **268**, (2000) 50.

[44] R. Carretero-González, J. D. Talley, C. Chong and B. A. Malomed, Multistable solitons in the cubic-quintic discrete nonlinear Schrödinger equation, *Physica D* **216**, (2006) 77.

[45] F. Palmero, R. Carretero-González, J. Cuevas, P. G. Kevrekidis and W. Królikowski, Solitons in one-dimensional nonlinear Schrödinger lattices with a local inhomogeneity, *Phys. Rev. E* **77**, (2008) 036614.

M. A. Porter, R. Carretero-González, P. G. Kevrekidis, B. A. Malomed, Nonlinear lattice dynamics of Bose–Einstein condensates, *Chaos* **15**, (2005) 015115.

[46] R. Carretero-González, A Map Approach to Stationary Solutions of the DNLS Equation In: *The Discrete Nonlinear Schrödinger Equation*. Springer Tracts in Modern Physics, vol 232. Springer, Berlin, Heidelberg (2009) <https://doi.org/10.1007/978-3-540-89199-4-11>

[47] A. B. Togueu Motcheyo, C. Tchawoua, M. Siewe Siewe and J. D. Tchinang Tchameu, Multisolitons and stability of two hump solitons of upper cutoff mode in discrete electrical transmission line, *Phys. Lett. A* **375**, (2011) 1104.

[48] M. Johansson, G. Kopidakis, S. Lepri and S. Aubry, Transmission thresholds in time-periodically driven nonlinear disordered systems, *EPL*, **86**, (2009) 10009.

[49] D. Cubero, J. Cuevas, and P. G. Kevrekidis, Nucleation of breathers via stochastic resonance in nonlinear lattices, *Phys. Rev. Lett.* **102**, (2009) 205505.

[50] D. De Santis, C. Guarcello, B. Spagnolo, A. Carollo, D. Valenti, AC-locking of thermally-induced sine-Gordon breathers, *Chaos Sol. Fract.* **170** (2023) 113382.

[51] J. M. Soto-Crespo, N. Devine, and N. Akhmediev, Integrable turbulence and rogue Waves: breathers or solitons? *Phys. Rev. Lett.* **116**, (2016) 103901.

[52] [https://www.dickinson.edu/news/article/1681/rogue\\_pendulum](https://www.dickinson.edu/news/article/1681/rogue_pendulum)

[53] J.F.R. Archilla, Y. Doi, M. Kimura, Pterobreathers in a model for a layered crystal with realistic potentials: Exact moving breathers in a moving frame, *Phys. Rev. E* **100**, (2019) 022206.

J. Bajārs and J.F.R. Archilla, Frequency-momentum representation of moving breathers in a two dimensional hexagonal lattice, *Physica D* **441**, (2022) 133497.

J.F.R. Archilla and J. Bajārs, Spectral properties of exact polarobreathers in semiclassical systems, *Axioms* **12**, 5 (2023) 437.